Dissipation of Intersubband Plasmons in Wide Quantum Wells

J. B. Williams,[1] M. S. Sherwin,[1] K. D. Maranowski,[2] and A. C. Gossard[2]
[1]*Department of Physics, University of California, Santa Barbara, California 93106*
[2]*Department of Materials, University of California, Santa Barbara, California 93106*
(Received 13 December 2000; published 2 July 2001)

This Letter reports detailed measurements of the dissipation times τ_d of ~10 meV intersubband (ISB) plasmons, and of the (single-particle) transport lifetimes τ_μ, in a remotely doped 40 nm GaAs quantum well. Introduced here as the time for ISB plasmons to dissipate into other modes of the electron gas, τ_d is deduced from the homogeneous ISB absorption linewidth, measured as a function of sheet concentration and perpendicular dc electric field. Modeling in this and the next Letter [C. A. Ullrich and G. Vignale, Phys. Rev. Lett. **87**, 037402 (2001)] indicates that scattering from rough interfaces dominates τ_d, while scattering from ionized impurities dominates τ_μ.

DOI: 10.1103/PhysRevLett.87.037401 PACS numbers: 78.67.De, 73.20.Mf, 73.21.Fg, 73.50.Dn

In a doped quantum well, confinement of electrons breaks the continuum of conduction band states into subbands [1]. The optically excited intersubband (ISB) excitation is known to be a collective mode of the 2D electron gas (2DEG), the ISB plasmon. The ISB plasmon can be thought of as a coherent superposition of single-particle intersubband excitations, with an energy renormalized from the bare intersubband spacing by Coulomb and exchange effects [1]. In the absence of processes like phonon emission, which remove energy from the electron gas, the width of a homogeneously broadened ISB absorption line is solely determined by the rate at which the collective mode dissipates into other modes of the 2DEG. Both disorder and a recently proposed intrinsic viscosity of the 2DEG [2,3] are expected to contribute to the ISB plasmon's dissipation, as described in detail in the next Letter [4].

Although much of the basic physics of the ISB excitation is well understood, there has so far been no microscopic theory of the linewidth. It is widely believed that the absorption line is homogeneously broadened in samples of high quality [1], and therefore due to scattering effects. Most of the experimental work has been done on wells less than 10 nm wide, which have transition energies in the mid-IR (~100 meV). Here, rapid emission of ~36 meV optical phonons contributes to the ISB linewidth [1,5–7], along with various types of disorder scattering. Because of ionized impurity scattering, the mid-IR ISB linewidth has been found to be larger for quantum wells doped in the well than in remotely doped quantum wells [8]. In remotely doped quantum wells, the mid-IR ISB linewidth is relatively insensitive to alloy disorder (which does degrade the mobility), but increases with decreasing well width [5]. The dependence on well width is consistent with a linewidth dominated by interface roughness (IFR) scattering. Experiments on InAs quantum wells show linewidths much smaller than would be expected based on nonparabolicity in a single-particle picture [7], and a very weak dependence on temperature [7], indicating the importance of the collective nature of the intersubband transition.

For wide GaAs quantum wells, with transitions far below the optical phonon energy, the ISB linewidth should be dominated by dissipation. At low temperatures (for example, 10 K) optical phonon emission is energetically forbidden and acoustic phonon emission is 2 orders of magnitude slower [9] than relevant time scales. Nonparabolicity is also negligible.

In this Letter, we present detailed measurements of the linewidth [10] and mobility of THz-frequency ISB excitations in a remotely doped 40 nm GaAs quantum well. For the first time in an intersubband absorption measurement, charge density and applied dc field are varied independently. Surprisingly, the linewidth depends more strongly on dc field than on charge density, increasing strongly as the sample is biased away from flat-band conditions. This field dependence clearly demonstrates that the line is homogeneously broadened, with its width dominated by IFR scattering away from flat band. The mobility, dominated by scattering of single particles, has completely different field- and charge-density dependences than the linewidth. Modeling indicates the mobility is dominated by scattering from ionized impurities. In the next Letter, our data are compared in detail with a new microscopic theory of the linewidth based on Refs. [2,3].

The sample studied was a 40 nm GaAs square well, grown by molecular beam epitaxy on a semi-insulating substrate. The conduction band edge profile is shown in Fig. 1. The sample consists of 100 nm GaAs, 180 nm superlattice (30 periods of 3 nm GaAs, 3 nm $Al_{0.3}Ga_{0.7}As$), 100 nm $Al_{0.3}Ga_{0.7}As$, Si delta-doped layer of charge concentration 5×10^{11} cm^{-2}, 10 nm $Al_{0.3}Ga_{0.7}As$ barrier, 8.5 nm GaAs quantum-well back gate, a barrier and doping layer identical to the above, 490 nm $Al_{0.3}Ga_{0.7}As$, Si delta-doped layer of charge concentration 3×10^{11} cm^{-2}, 100 nm $Al_{0.3}Ga_{0.7}As$ barrier, 40 nm GaAs quantum well, 100 nm $Al_{0.3}Ga_{0.7}As$ barrier, Si delta-doped layer of charge concentration 1×10^{12} cm^{-2}, 90 nm $Al_{0.3}Ga_{0.7}As$,

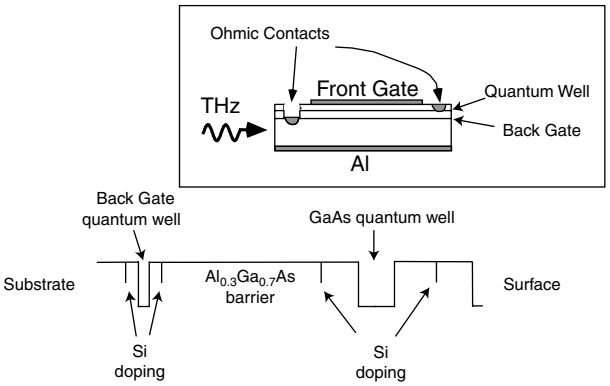

FIG. 1. Conduction band edge profile of the sample. The back gate is a narrow delta-doped quantum well which has no resonances in the THz. A wide barrier separates the back gate from the quantum well. Inset: Cross-section view of the processed sample. Separate Ohmic contacts were made to the back gate and quantum well on a 6 mm square sample. A 200 nm thick Al Schottky contact was evaporated onto the surface of the sample, on a 6 mm $\times$ 4 mm rectangular area, forming the front gate. Separate control of the gate voltages allows independent control of the charge density and dc electric field in the well. Another layer of Al was evaporated onto the back side of the sample, so that the Al layers on both sides of the sample form a waveguide. The absorption measurement was performed in the edge-coupling geometry, with the THz radiation coupled into the waveguide by a Winston cone (not shown).

and a 10 nm GaAs capping layer. The back gate is a narrow, doped quantum well which has no resonances at the frequencies of interest and was used to control the charge density in the wide quantum well (hereafter, "the quantum well") via the field effect. There are several conduction subbands in the wide quantum well, and the energy separation of the lowest two subbands is field tunable over a range of 10–20 meV. In this work, only the lowest subband was occupied, and only transitions between the lowest two subbands were measured.

The experiments were carried out at a temperature of 2.3 K. The charge density was determined by measuring the capacitance between the front gate and the quantum well as a function of the front gate voltage, and integrating to find the charge density. The procedure is repeated for different back gate voltages, and the resulting data tell us how to vary the two gate voltages simultaneously in order to vary the field while holding the density fixed, or vice versa. This measurement is not sensitive to charges localized by disorder. We estimate the density of localized charges to be of the order 1×10^{10} cm^{-2}.

The dc electric field is calculated from the applied gate voltages and sample dimensions. The calculation gives the field applied to the well by external charges on the gates and excludes any built-in electric field caused by static charges in the structure as well as bending of the bands due to electron-electron interaction (which is taken into account when the electron wave functions are calculated self-consistently in the mobility simulation).

The mobility was measured on a separate sample cleaved from an adjacent spot of the same wafer. The mobility sample was processed in the van der Pauw geometry [11], with a front gate over an active region of dimensions 2 mm $\times$ 2 mm. The density and field were determined as described above for the THz absorption sample.

The spectra were measured with a FT-IR spectrometer, using the edge-coupling geometry, as shown in the inset in Fig. 1. The THz radiation was concentrated on the edge of the sample using a Winston cone. The path length through the sample was 6 mm. A polarizer inserted after the sample selected that component of the transmitted light with polarization in the growth direction, which was then detected by a bolometer. Each raw spectrum, measured with electrons in the well, was normalized to a spectrum measured with the well depleted of electrons by the gates. The resulting attenuation coefficient is given by

$$\alpha(\omega) = \frac{1}{\text{sample length}} \ln \frac{I(\text{empty})}{I(\text{full})},$$

where ω is the frequency, I(empty) is the transmitted intensity vs frequency with the well depleted of electrons, and I(full) is the transmitted intensity vs frequency with the well full of electrons.

Typical spectra, measured for several values of the applied field, at a constant charge density of 5×10^{10} cm^{-2}, are shown in Fig. 2. The linewidth shows an unexpectedly sharp minimum at zero field and saturates with a larger value at nonzero field. From a fit of the normalized absorption spectrum to a Lorentzian, we obtain the peak position and linewidth of the absorption curve. The peak positions are plotted against applied dc field, for several values of the charge density, in Fig. 3a. The peak position is widely tunable, from 75 to over 160 cm^{-1}. Since this is a symmetric quantum well, the peak position is expected to be symmetric about its minimum value at zero dc field. The

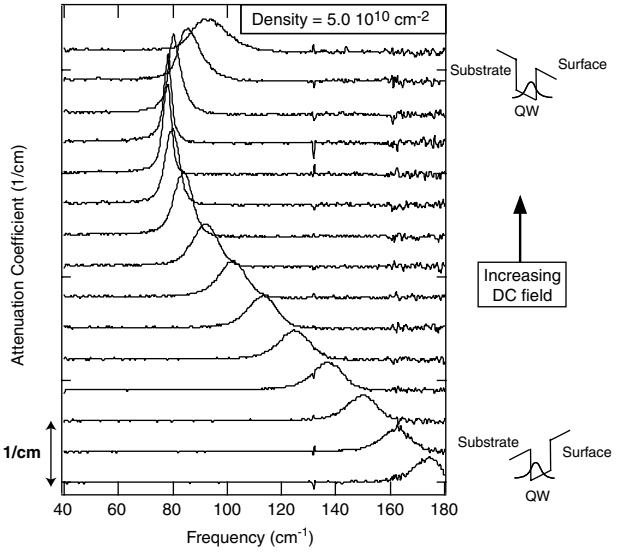

FIG. 2. Typical normalized absorption spectra at several values of the electric field. The density for these spectra was held constant at 5×10^{10} cm^{-2}. The field can be seen to go through flat-band (where the peak position is at a minimum). The line dramatically narrows at flat-band.

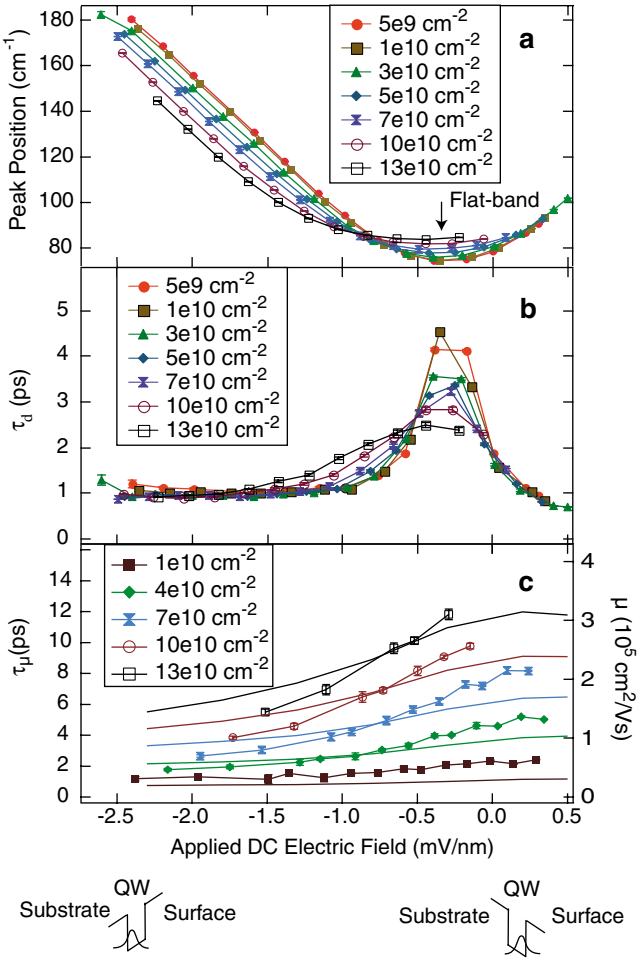

FIG. 3 (color). (a) Absorption peak position vs field for several values of density. The data are well fit by calculations (not shown). The minimum in the peak position should occur where the field inside the well is zero. The offset of the minimum away from zero applied field is due to a constant built-in field in the sample. (b) ISB dissipation time [$\tau_d = (2\pi c \times \text{linewidth})^{-1}$] vs field for several values of density. A sharp maximum in τ_d occurs at flat-band. (c) Mobility lifetime (τ_μ) data (points) and calculation (lines) vs field for several values of density. The mobility lifetimes are longer than the intersubband dissipation times, and the trends do not correlate, implying that the several scattering mechanisms affect linewidth and mobility differently. Scattering from bulk impurities in the well at the level of roughly 10^{15} cm^{-3} dominates the simulated mobility. The field dependence of the mobility is caused by a position-dependent bulk impurity profile, which is due to dopant segregation during growth.

peak position is symmetric about a minimum which occurs at an applied field of -0.3 mV/nm, which implies that the structure has an additional fixed, built-in field of $+0.3$ mV/nm.

The existence of a sharp minimum at flat-band in the field dependence of the linewidth, seen in Fig. 2, cannot be explained by assuming that the line is inhomogeneously broadened. With the remote donor layers 100 nm away from the well, the most likely source of inhomogeneous broadening is inhomogeneity of the width of the well over a macroscopic length scale. Such inhomogeneity would cause intersubband plasmons in different parts of the sample to absorb at different frequencies. However, this inhomogeneity would be weakest away from flat-band, when electrons everywhere in the plane are pushed against one side of the well and feel a potential which is triangular, independent of the position of the other side of the well. This would lead to a maximum in the linewidth at flat-band, which is the opposite of what we observe. Thus, the line is homogeneously broadened, and therefore the linewidth is inversely proportional to the dissipation time τ_d of the excitation, which is determined by scattering. The linewidth (half width at half maximum) is related to the dissipation time by $\tau_d = (2\pi c \times \text{linewidth})^{-1}$.

The ISB dissipation time is plotted against applied dc field in Fig. 3b. The data show several interesting features. First, the dissipation time has a strong field dependence, having a sharp maximum at zero bias, which coincides with the minimum in peak position. Second, the field dependence is greater at low charge densities than at high charge densities. Third, the dissipation time data are asymmetric about zero field, saturating at 1 ps for negative field (more negative front gate) but appearing lower than that for positive field (more positive front gate).

The in-plane mobility is plotted in Fig. 3c. The mobility was actually anisotropic; we have plotted the geometric mean of the two in-plane components of the mobility tensor. The mobility does not show a maximum at flat-band and is indeed uncorrelated to the intersubband dissipation time. The mobility also shows an asymmetry about flat-band, being higher for positive field than for negative field.

We interpret both the ISB dissipation and mobility data in terms of scattering from disorder in the well. Unlike in the case of an ensemble of molecules or atoms [12], static disorder can be a source of homogeneous broadening for collective modes like ISB plasmons: such disorder can cause the plasmon to scatter into other modes of the 2DEG. The main sources of disorder in the GaAs/$Al_{0.3}Ga_{0.7}As$ quantum well are ionized impurities in the delta-doping layers, interface roughness, alloy disorder in the $Al_{0.3}Ga_{0.7}As$ barriers, and bulk impurities in the well. Remote impurities are far enough from our well to have little influence. Because of the short-range nature of the IFR and alloy disorder potentials, one expects scattering from such potentials to be strong only when the wave functions strongly overlap with the interface and penetrate the barriers, as is the case away from flat-band. Thus, the IFR and alloy disorder scattering rates are greatly decreased at flat-band. The bulk impurity distribution is largely due to the segregation of impurities from the delta-doped layer during growth [13]. It is monotonically decreasing in the growth direction and can extend into the well. When a negative field is applied to the well, electrons are pushed towards the substrate and experience a higher local impurity density. Thus, bulk impurity scattering is greater at negative fields than at positive fields.

The field dependence of the data indicates which scattering mechanisms determine the ISB plasmon dissipation

and the mobility. The peak in the dissipation time at flat band is consistent with IFR or alloy disorder scattering. Reference [5] indicates that alloy disorder can be ignored, so we conclude that the ISB plasmon dissipation is dominated by IFR scattering. The expected field dependence of the bulk impurity scattering rate qualitatively explains the asymmetry in the field dependence of the mobility, as seen in Fig. 3c.

We checked that our explanation of the mobility data is quantitatively correct by calculating the transport scattering rate in the Born approximation, including quasi-2D linear Thomas-Fermi screening (Fig. 3c). The electronic wave functions were plane waves in the plane of the quantum well, multiplied by a growth-direction-dependent envelope function calculated self-consistently in the Hartree approximation. The IFR scattering potential was calculated after Ref. [14], assuming Gaussian-correlated roughness characterized by an average height $\Delta = 0.4$ nm and correlation length $\xi = 6.44$ nm (parameters which best fit the linewidth in Ref. [4]). Scattering from remote ionized impurities in the delta-doped layers was calculated assuming sheet density of 4.8×10^{11} cm^{-2} in the upper layer. The lower layer was treated as a bulk distribution which had segregated towards the surface during growth. Scattering from these bulk impurities was calculated after Ref. [15], assuming a distribution given by $\rho(z) = 1.33 \times 10^{15} \times e^{-z/30\,\mathrm{nm}}$ cm^{-3}, where the zero of z lies in the center of the well. This distribution was chosen to give a reasonable fit to the mobility data and is consistent with measured distributions reported by other authors [13]. The mobility calculation is dominated by scattering from the bulk impurities.

In conclusion, we have carried out a detailed measurement of the mobility and intersubband linewidth of electrons in a quantum well, in which we vary the charge density and dc electric field independently. The field dependence of the linewidth shows that the line is homogeneously broadened and dominated by IFR scattering. The field dependence of the mobility shows that it is dominated by scattering from bulk impurities in the well. Our data will be useful for a detailed comparison to a new microscopic theory of the ISB linewidth, as well as in the design of THz devices based on ISB transitions.

The authors acknowledge useful discussions with C. A. Ullrich, C. Kadow, and D. Jena. This work was funded by NSF-DMR, AFOSR, and ONR-MFEL.

[1] M. Helm, in *Intersubband Transitions in Quantum Wells: Physics and Device Applications I,* edited by H. C. Liu and F. Capasso, Semiconductors and Semimetals Vol. 62 (Academic Press, San Diego, 2000), pp. 1–99.
[2] G. Vignale, C. A. Ullrich, and S. Conti, Phys. Rev. Lett. **79**, 4878 (1997).
[3] C. A. Ullrich and G. Vignale, Phys. Rev. B **58**, 15 756 (1998).
[4] C. A. Ullrich and G. Vignale, Phys. Rev. Lett. **87**, 037402 (2001).
[5] K. L. Campman, H. Schmidt, A. Imamoglu, and A. C. Gossard, Appl. Phys. Lett. **69**, 2554 (1996).
[6] J. Faist, C. Sirtori, F. Capasso, L. Pfeiffer, and K. W. West, Appl. Phys. Lett. **64**, 872 (1994).
[7] R. J. Warburton, K. Weilhammer, J. P. Kotthaus, M. Thomas, and H. Kroemer, Phys. Rev. Lett. **80**, 2185 (1998).
[8] E. B. Dupont, D. Delacourt, D. Papillon, J. P. Schnell, and M. Papuchon, Appl. Phys. Lett. **60**, 2121 (1992).
[9] J. N. Heyman, K. Unterrainer, K. Craig, B. Galdrikian, M. S. Sherwin, K. Campman, P. F. Hopkins, and A. C. Gossard, Phys. Rev. Lett. **74**, 2682 (1995).
[10] A preliminary account of the linewidth measurements can be found in J. B. Williams, M. S. Sherwin, K. D. Maranowski, C. Kadow, and A. C. Gossard, Physica (Amsterdam) **7E**, 204 (2000).
[11] A. A. Ramadan, R. D. Gould, and A. Ashour, Thin Solid Films **239**, 272 (1994).
[12] S. Mukamel, *Principles of Nonlinear Optical Spectroscopy* (Oxford University Press, Oxford, 1995).
[13] L. Pfeiffer, E. F. Schubert, K. W. West, and C. W. Magee, Appl. Phys. Lett. **58**, 2258 (1991).
[14] G. Fishman and D. Calecki, Phys. Rev. Lett. **62**, 1302 (1989).
[15] L. Hsu and W. Walukiewicz, Phys. Rev. B **56**, 1520 (1997).